J. Org. Chem. **2001,** *66,* 2449−2458

Modeling the 1,3-Dipolar Cycloaddition of Nitrones to Vinylboranes in Competition with Boration, Cyclization, and Oxidation Reactions

Augusto Rastelli,*,† Remo Gandolfi,‡ Mirko Sarzi-Amadé,‡ and Bertrand Carboni§

Dipartimento di Chimica, Università di Modena, 41100 Modena, Via Campi 183, Italy,
Dipartimento di Chimica Organica, Università di Pavia, 27100 Pavia, Via Taramelli 10, Italy, and
Synthèse et Electrosynthèse Organiques,UMR CNRS 6510, Campus de Beaulieu,
Avenue du Général Leclerc, 35042 Rennes Cedex, France

rastelli@unimo.it

Received December 28, 2000

Structures and energetics of reactants, reactant complexes, concerted transition structures, and products of the cycloaddition of the prototypical nitrone with vinylborane have been produced and discussed. Structure optimizations have been performed at the B3LYP/6-31G(d) and B3LYP/AUG-cc-pVDZ levels of approximation, and single-point calculations on the B3LYP geometries have been carried out at the MP4(SDTQ) level with the same basis sets. Kinetic contributions to standard enthalpies, entropies, and free enthalpies have been computed at the same levels of geometry optimizations. The effects of methyl and chloro substitution on the BH_2 group and of methyl substitution on the vinyl moiety has been also explicitly considered. The most striking theoretical features of this cycloaddition are (i) the formation of reactant complexes where the nitrone oxygen is strictly bound up to the boron atom (B···O interactions), (ii) their persistence in the endo/exo transition structures, and (iii) energy profiles suggesting very high reaction rates, regiospecificity (5-borylisoxazolidines) and complete endo-stereoselectivity. The BH_2 (BX_2) substituent appears to induce a sort of intramolecular catalysis which is also largely selective in favor of the endo reaction path. Possible competitive reaction paths such as cyclization, organoboration, and oxidation have equally been investigated, on the same grounds, both with prototypical reagents and with dimethylvinylborane, dichlorovinylborane, 2-methyl-1-propenylborane, and 2-methyl-1-propenyldichloroborane. The transition structures for these reaction paths are significantly higher in energy than those of the corresponding 1,3-dipolar cycloadditions in the sequence oxidation ≫ cyclization > boration > cycloaddition, whereas the resulting reaction products show the reversed sequence. Polar solvents appear to increase the competition of boration although maintaining its character of secondary reaction. As expected, the reaction rate of 1,3-dipolar cycloaddition is lowered by dimethyl substitution on the vinyl CH_2 reacting center (i.e., for the reaction of 2-methyl-1-propenylborane and 2-methyl-1-propenyldichloroborane) whereas the reaction rate of boration is increased, the boration results being significantly competitive even in the gas phase. Experiments for the control of the above predictions are not yet available.

Introduction

From the experimental point of view, the cycloaddition of nitrones with olefins is one of the most studied reactions, among all the 1,3-dipolar cycloadditions.[1] It provides the most efficient method to prepare isoxazolidines that are widely used as starting compounds in organic synthesis, in particular for building natural products.[2] We have long been engaged in studying the mechanism of nitrone cycloaddition, and our main interest has been focused in assessing the factors that control regiochemistry and endo/exo selectivity, in defining the role played by secondary interactions, and in exploring the levels of calculations able to account for the experimental behavior in this class of reactions.[3] As a fact, experimental activation thermodynamic parameters and product selectivities of a few well-explored nitrone cycloadditions appeared to be fairly well reproduced by standard theoretical calculations limited to the reactions of the prototypical nitrone (nitrone), provided that high levels of electron correlation were introduced, either with the use of Density Functional procedures or with the post-SCF Moeller−Plesset perturbation technique.[3c] On these grounds, we deemed it reasonably safe to attempt a theoretical study on the unknown cycloadditions of nitrones with vinylboranes.

As far as we know, the 1,3-dipolar cycloaddition using vinylboranes as dipolarophiles does not seem to have

---

* To whom correspondence should be addressed. Phone: +39-059-2055080. Fax: +39-059-373543.

† Università di Modena.

‡ Università di Pavia.

§ Synthèse et Electrosynthèse Organiques.

(1) Tufariello, J. J. *Nitrones in 1,3-Dipolar Cycloaddition Chemistry*; Padwa A., Ed.; Wiley-Interscience: New York; 1984; Vols. 1−2.

(2) Grünanger, P.; Vita Finzi, P. *Isoxazoles*; Wiley-Interscience: New York; 1991 and 1999; Parts 1 and 2.

(3) (a) Burdisso, M.; Gamba, A.; Gandolfi, R. *Tetrahedron* **1988**, *44*, 3735. (b) Burdisso, M.; Gandolfi, R.; Grünanger, P.; Rastelli, A. *J. Org. Chem.* **1990**, *55*, 3427. (c) Rastelli, A.; Gandolfi, R.; Sarzi-Amadè, M. Regioselectivity and Diastereoselectivity in the 1,3-Dipolar Cycloadditions of Nitrones with Acrylonitrile and Maleonitrile. The Origin of the Endo/Exo Selectivity. In *Advances in Quantum Chemistry*; Academic Press: London, 2000; Vol. 35, p 151. (d) Di Valentin, C.; Freccero, M.; Gandolfi, R.; Rastelli, A. *J. Org. Chem.* **2000**, *65*, 6112. (e) Rastelli, A.; Gandolfi, R.; Di Valentin, C., manuscript in preparation.

10.1021/jo001801n CCC: $20.00

been given any attention, and only a few experimental studies have been reported for the cycloaddition of diazoalkanes,[4] nitrile oxides,[5] and nitrones to vinylboronic esters.[6] On the contrary, in the past decade the Diels−Alder reaction with vinylboranes has been extensively studied, both experimentally and theoretically, mainly by the Singleton's group,[7] and the peculiar reactivity of vinylboranes (anomalously high and relatively invariant with electron-rich, electron-poor, and unactivated dienes) has been smartly rationalized as the effect of an original secondary interaction between the boron atom and a terminal carbon atom of the diene moiety. It is worthy of note that much of the experimental research has been preceded or has received definite impulse by the theoretical prediction of unexpected (4 + 3 atoms) transition structures where the boron atom is intimately involved in the pericyclic transition state.[8] It appeared interesting to investigate whether these kinds of interactions and transition structures were also active in nitrone cycloadditions and were able to affect reaction rates and product distributions, i.e., regioselectivity and endo/exo diastereoselectivity of these reactions.

We started by studying the concerted cycloaddition of the prototypical nitrone with vinylborane. Since our former results strongly suggested high reaction rates and complete regio/diastereoselectivity of the reaction products (the optimal features for the practical usefulness of the reaction), we were even more surprised of the absence of experimental reports in the extant literature, although we could not exclude that this absence could be ascribed to the fact that other reactions might occur between the same reactants so as to prevent or override the 1,3-dipolar cycloaddition. In less recent literature,[9] in fact, some boration reactions between nitrones and BR_3 (R = Me, Et, Pr, ^{i}Pr, Ph) have been described, but no reaction appears to have been reported between nitrones and vinylboranes. Moreover, under the real conditions of the experimental tests (substituted nitrones in the place of the prototypical one, substituted vinylboranes, solution in the place of gas phase, etc.) the “prototypical theoretical reaction paths” could be significantly modified. In part, these problems were tentatively explored (i) by studying vinylboration, oxidation, and (3 + 3 atoms) cyclization, (ii) by considering simple substituted vinylboranes, i.e. dichlorovinylborane, dimethylvinylborane, 2-propenylborane, 2-methyl-1-propenylborane, and 2-methyl-1-propenyldichloroborane, and (iii) by performing a rough evaluation of solvent effects.

Methods

Geometries for all the stationary structures along the concerted reaction paths were fully optimized at the B3LYP/6-31G(d) (in short, MOD1) and B3LYP/AUG-cc-pVDZ, (MOD2), levels of theory utilizing gradient geometry optimization and default threshold for convergence, as implemented in the GAUSSIAN 98 series of programs.[10] Stationary points were fully characterized as minima or first-order saddle points by diagonalizing the Hessian matrixes of the optimized structures. All the transition structures were found to have only one negative eigenvalue, the corresponding eigenvector having the form of the expected reaction mode. All the wave functions were tested for all instabilities and found to be stable. Single-point MP4(SDTQ) energy calculations were done on the MOD1 and MOD2 optimized structures.

In most cases Intrinsic Reaction Coordinate (IRC)[11] calculations starting at the saddle points were done to verify the connections between the transition structures and their preceding and following minima along the reaction path. The magnitude of Basis Set Superposition Errors (BSSE) was evaluated with counterpoise calculations[12] using ghost atoms, and found to not affect the qualitative aspect of the energy profiles. NBO (Natural Bond Orbital)[13] calculations were performed for a preliminary evaluation of the interactions between the boron atom of the dipolarophile and the terminal atoms of nitrone, and for the evaluation of the forming bonds.

Solvent effects were tested using the Polarized Continuum Model (PCM) of Tomasi and co-workers[14] and the CPCM version of Barone and co-workers.[15] Zero-point energy, enthalpy, entropy, and free enthalpy were also calculated within the ideal gas, rigid rotor, and harmonic oscillator approximations (1 atm and 298.15 K). The entropic effects of the statistical reaction factors were also included. Entropy, enthalpy, and free enthalpy values were converted into the standard state of molar concentration for a direct comparison with the experimental results in solution where the same activity scale is generally used.

Results and Discussion

Summarized in Scheme 1 are the reaction paths, connected in a complex pattern,[16] studied in detail in the following sections. The reactants in proper orientations could lead to A-TS's (via path a) evolving toward A-regioadducts (4-borylisoxazolidines) and to B-TS's (via path b) evolving toward B-regioadducts (5-borylisoxazo-

---

[4] (a) Matteson, D. S. *J. Org. Chem.* **1962**, *27*, 4293. (b) Woods, W. G.; Bengeldof, I. S. *J. Org. Chem.* **1966**, *31*, 2769. (c) Jazouli, M.; Carboni, B.; Carrié, R.; Soufiaoui, M.; Toupet, L. *Heteroatom. Chem.* **1994**, *5*, 513.

[5] (a) Wallace, R. H.; Zong, K. K. *Tetrahedron Lett.* **1992**, *33*, 6941. (b) Wallace, R. H.; Liu, J. *Tetrahedron Lett.* **1994**, *35*, 7493. (c) Liu, J.; Eddings, A.; Wallace, R. H. *Tetrahedron Lett.* **1997**, *38*, 6971 and 6795. (d) Wallace, R. H.; Zong, K. K.*J. Organomet. Chem.* **1999**, *581*, 87. (e) Jazouli, M.; Baba, S.; Carboni, B.; Carrié, R.; Soufiaoui, M. *J. Organomet. Chem.* **1995**, *498*, 229. (f) Marsden, S. P.; Stokes, E. A. S. *Tetrahedron Lett.* **1998**, *39*, 8513.

[6] (a) Carboni, B.; Ollivault, M.; Le Bouguenec, F.; Carrié, R.; Jazouli, M. *Tetrahedron Lett.* **1997**, *38*, 6665. (b) Davies, C. D.; Marsden, S. P.; Stokes, E. S. *Tetrahedron Lett.* **2000**, *41*, 4229.

[7] Singleton, D. A. *Advances in Cycloaddition*; JAI Press: Greenwich, CT, 1997; Vol 4, p 121 and literature cited therein.

[8] (a) Singleton, D. A.; Leung, S.-W.*J. Org. Chem.* **1992**, *57*, 4796. (b) Singleton, D. A. *J. Am. Chem. Soc.* **1992**, *114*, 6563.

[9] Paetzold, P.; Schimmel, G. *Z. Naturforsch.* **1980**, *35b*, 568.

[10] Frisch, M. J.; Trucks, G. W.; Schlegel, H. B.; Scuseria, G. E.; Robb, M. A.; Cheeseman, J. R.; Zakrzewski, V. G.; Montgomery, J. A.; Stratmann, R. E.; Burant, J. C.; Dapprich, S.; Millam, J. M.; Daniels, A. D.; Kudin, K. N.; Strain, M. C.; Farkas, O.; Tomasi, J.; Barone, V.; Cossi, M.; Cammi, R.; Mennucci, B.; Pomelli, C.; Adamo, C.; Clifford, S.; Ochterski, J.; Petersson, G. A.; Ayala, P. Y.; Cui, Q.; Morokuma, K.; Malick, D. K.; Rabuck, A. D.; Raghavachari, K.; Foresman, J. B.; Cioslowski, J.; Ortiz, J. V.; Stefanov, B. B.; Liu, G.; Liashenko, A.; Piskorz, P.; Komaromi, I.; Gomperts, R.; Martin, R. L.; Fox, D. J.; Keith, T.; Al-Laham, M. A.; Peng, C. Y.; Nanayakkara, A.; Gonzales, C.; Challocombe, M.; Gill, P. M. W.; Johnson, B. J.; Chen, W.; Wong, M. J.; Andres, J. L.; Head-Gordon, M.; Replogle, E. S.; Pople, J. A. *Gaussian 98* , Revision A.7, Gaussian, Inc., Pittsburgh, PA, 1998.

[11] (a) Fukui, K. *Acc. Chem. Res.* **1981**, *14*, 363. (b) Gonzales, C.; Schlegel, H. B. *J. Phys. Chem.* **1989**, *90*, 2154. (c) Gonzales, C.; Schlegel, H. B. *J. Phys. Chem.* **1990**, *94*, 5523.

[12] (a) Schwenke, D. W.; Truhlar, D. G. *J. Chem. Phys.* **1985**, *82*, 2418. (b) Frisch, M. J.; Del Bene, J. E.; Binkley, J. S.; Schaefer, H. F., III. *J. Chem. Phys.* **1986**, *84*, 2279.

[13] Glendening, E. D.; Reed, A. E.; Carpenter, J. E.; Wheinhold, F. NBO version 3.1.

[14] (a) Miertus, S.; Scrocco, E.; Tomasi, J. *Chem. Phys.* **1981**, *55*, 117. (b) Miertus, S.; Tomasi, J. *Chem. Phys.* **1982**, *65*, 239.

[15] Barone, V.; Cossi, M. *J. Phys. Chem.* A **1998**, *102*, 1995.

[16] All the paths described in Scheme 1 are probable on the grounds of general information. In particular, path g (including alkyl or vinyl migration) and path e (including alkyl migration) can be related to examples given in Valtier, M.; Carboni, B. In *Comprehensive Organometallic Chemistry II*; Wilkinson, G., Stone, F. G. A., Abel, E. W., Eds.; Pergamon Press: Oxford, 1995; Vol. 11, p 191. A structure related to **Oxi-P** has been very recently described in Chen, G.-M.; Brown, H. C. *J. Am. Chem. Soc.* **2000**, *122*, 4217. A related example for path f can be found in Petasis, N. A.; Zavialov, I. A. *Advances in Boron Chemistry*; Siebest, W., Ed.; Royal Chemical Society: Cambridge, 1997; p 179.

Scheme 1

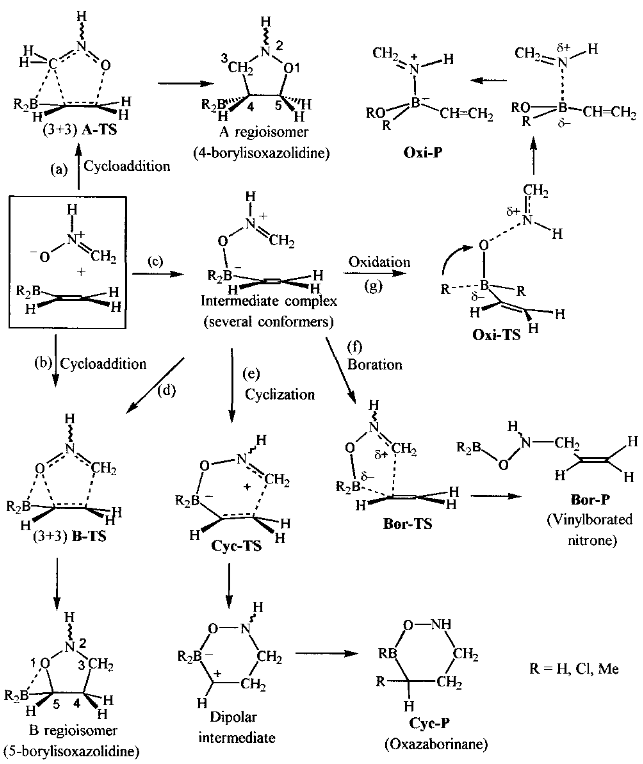

Scheme 2

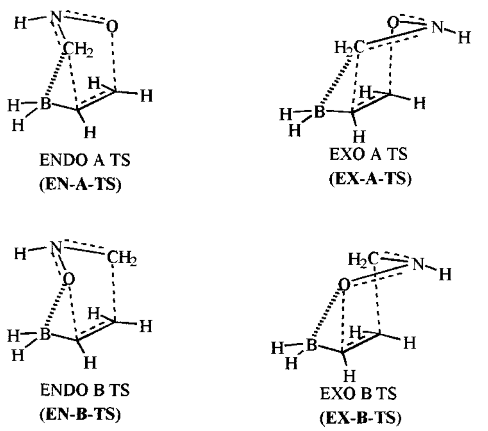

lidines). Given the relatively high basicity of nitrones, one can anticipate the easy formation of a relatively stable intermediate complex (via path c) in various conformations. This intermediate can then partition among at least four pathways: (i) intramolecular cycloaddition (via path d), once again involving the B-TS's; (ii) cyclization (via path e) to six-membered ring dipolar intermediates and finally to oxazaborinanes; (iii) 1,4-shift of the vinyl fragment (via path f, boration] leading to vinylborated nitrones; (iv) rearrangement with cleavage of the O−N bond, migration of R (via path g) (or of the vinyl group) to the oxygen atom and fragmentation to afford oxidated boranes and imine, possibly bound through a B−N bond. All of these pathways can take place according to at least two diastereisomeric TSs (e.g., endo/exo TSs for the 1,3-dipolar cycloaddition, Scheme 2).

We will discuss first the reactions between the prototypical reactants, i.e., nitrone and vinylborane.

Intermediate Complexes. Nitrone and vinylborane may undergo formation of a stable complex, in several conformations, where the boron atom is strongly bound to the nitrone oxygen. The three conformers reported in Figure 1 play a significant role in the description of the reaction mechanisms as illustrated in the following sections. The most stable conformer C is involved as an IRC connected "starting structure" in the oxidation reaction with vinyl migration, while **EN−B−C** and **EX−B−C** are IRC starting structures in all the other reactions.

1,3-Dipolar Cycloaddition. The cycloaddition of nitrone with ethene leads to a concerted transition structure via eight equivalent reaction paths; with monosubstituted alkenes four different transition structures can be expected, corresponding to the two different relations of the nitrone oxygen with respect to the substituted carbon of the alkene (i.e., B regiochemistry when the oxygen atom binds the substituted carbon leading to 5-substituted isoxazolidines, A regiochemistry when it binds the unsubstituted one leading to 4-substituted isoxazolidines) (Schemes 1 and 2), and to the two different diastereoisomeric relations of the N−H moiety with respect to the alkene substituent (endo/exo diastereochemistry, Scheme 2). The four reaction paths ENDO B, EXO B, ENDO A, EXO A each have a statistical reaction factor of 2 (i.e., there are two enantiomeric TSs for each path).

The two models for geometry optimizations and for kinetic contributions are called MOD1 = B3LYP/6-31G(d) and MOD2 = B3LYP/AUG-cc-pVDZ, whereas MP4/MOD1 stands for MP4/6-31G(d)//B3LYP/6-31G(d) and MP4/MOD2 for MP4/AUG-cc-pVDZ//B3LYP/AUG-cc-pVDZ.

Figure 2 presents the MP4/MOD1 and MP4/MOD2 (italics) energy (zero-point energy included) profiles corresponding to the four distinct concerted reaction paths of the cycloaddition of vinylborane with nitrone leading to isoxazolidines. Figures 1 and 3 collect the most relevant optimized critical structures appearing in Figure 2, whereas Table 1 collects structural information.

To simplify the descriptions we will consider explicitly only MOD1 stuctures and MP4/MOD1 energies. In the stable complexes, **EN−B−C** and **EX−B−C**, the boron atom and the nitrone oxygen are very tight, 1.641 and 1.600 Å, respectively; their Wiberg bond-indices[17] (Table 1) amount to 0.52 and 0.56, respectively, thus supporting the presence of strong B···O interactions and confirming that the interaction in **EX−B−C** is stronger than in **EN−B−C**.[18] In the **EN−B−TS** transition structure the B···O interaction becomes slightly stronger (1.630 Å, bond-index 0.55), whereas it becomes slightly weaker in **EX−B−TS** (1.613 Å, bond-index 0.55). One can observe that the **EX−B−TS** structure gets the same B···O bond-index as the **EN−B−TS** structure but at a significantly shorter interatomic distance (thus involving higher repulsive terms); actually, NLBO analysis[13] shows that the deviation of the natural hybrids from the line of B···O centers is larger in the former case (7.5°, 14.2°) than in the latter (3.0°, 10.3°). As a consequence, the EXO B approach to the transition structure is less supported by the B···O

---

(17) Wiberg, K. B. *Tetrahedron* **1968**, *24*, 1083, as formulated in terms of the Natural Atomic Orbital basis set. Wiberg bond index represents the sum of squares of off-diagonal density matrix elements between atoms.

(18) The strength of the interaction can be appreciated when considering that the B−O bond distances in boronic esters are about 1.38 Å (in the same model MOD1) with a bond-index of 0.91.

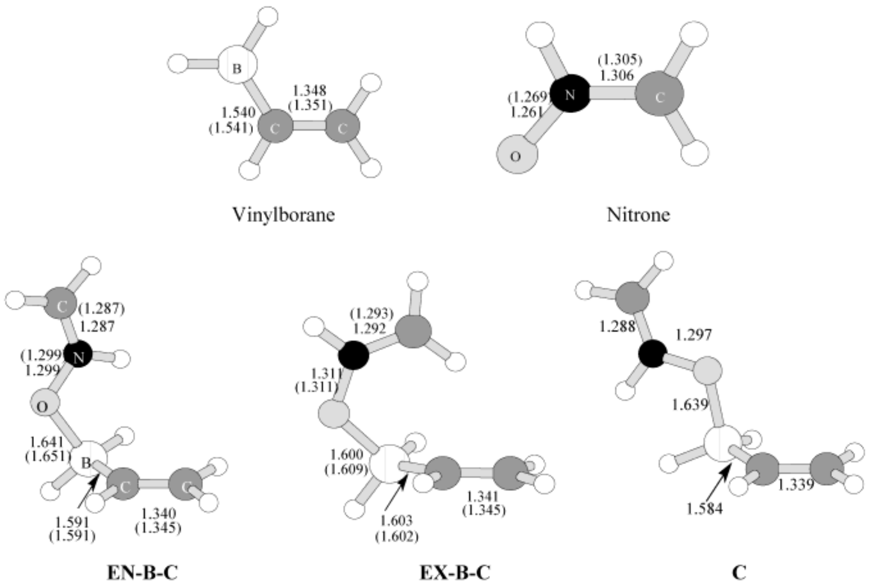

Figure 1. Optimized [B3LYP/6-31G(d), (MOD1)] vinylborane, nitrone, and nitrone−vinylborane complex structures. Bond lengths are in angstroms. In parentheses are reported the B3LYP/AUG-cc-pVDZ (MOD2) values.

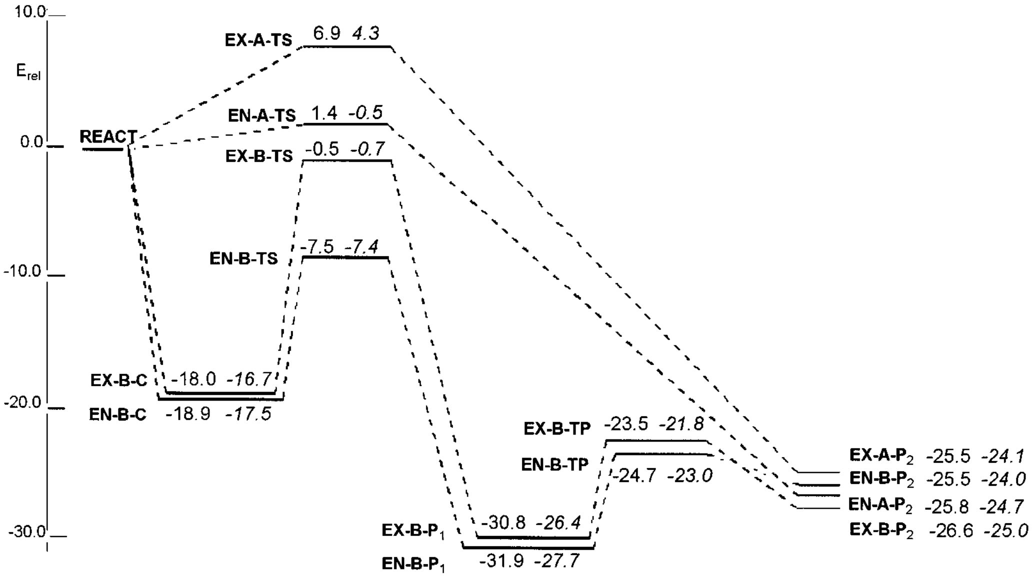

Figure 2. MP4(SDTQ)/6-31G(d)//B3LYP/6-31G(d) (MP4/MOD1) energy profile, including ZPE contributions, for the 1,3-dipolar cycloaddition of nitrone to vinylborane. In italics are reported the MP4(SDTQ)/AUG-cc-pVDZ//B3LYP/AUG-cc-pVDZ (MP4/MOD2) values.

interaction, **EX−B−TS** is less early, and its energy is much higher than that of **EN−B−TS**. The distances of the C···C and C···O forming bonds (Figure 3) and the increased energy difference of **EN−B−TS** and **EX−B−TS** with respect to **EN−B−C** and **EX−B−C** (Figure 2) agree with the above explanation. Noteworthy, the concerted transition structures are asynchronous (the C···C bonds resulting much more advanced than the C···O ones) and can be labeled as (3 + 3 atoms) transition structures instead of the regular (3 + 2 atoms) ones. Despite the fact that the B···O interactions are the largest interactions between the reacting fragments, the reaction traslational modes clearly show that the (3 + 3) transition structures do evolve toward the products **EN−B−P1** and **EX−B−P1** on one side and toward the reactant complexes **EN−B−C** and **EX−B−C**, on the other side; IRC (Intrinsic Reaction Coordinate) calculations confirm all the connections of Figure 2. It is interesting to observe that in the “intramolecular” cycloaddition of these B-TSs the nitrone fragment acts as the electrophilic partner and the vinylborane moiety is the nucleophilic component. Moreover, the favor for **EN−B-TS** over **EX−B−TS** stems from the very strong secondary interaction between the nitrone oxygen and the boron atom while there is not any evidence for the “classical” secondary interaction between the boron atom and the nitrone nitrogen.

The products **EN−B−P1** and **EX−B−P1** (Figure 3 and Table 1) show well formed C−C and C−O bonds, but also significant B···O interactions (1.698 Å, bond-index 0.43 for **EN−B−P1**; 1.676 Å, bond-index 0.45 for **EX−B−P1**). These structures may undergo conformational rearrangement through the transition structures **EN−B-TP** and **EX−B−TP** toward the less stable products **EN−B−P2** and **EX−B−P2**,[19] respectively. The main components of the rearrangement modes are the rotation of the BH_2 group and the increasing B···O distance.

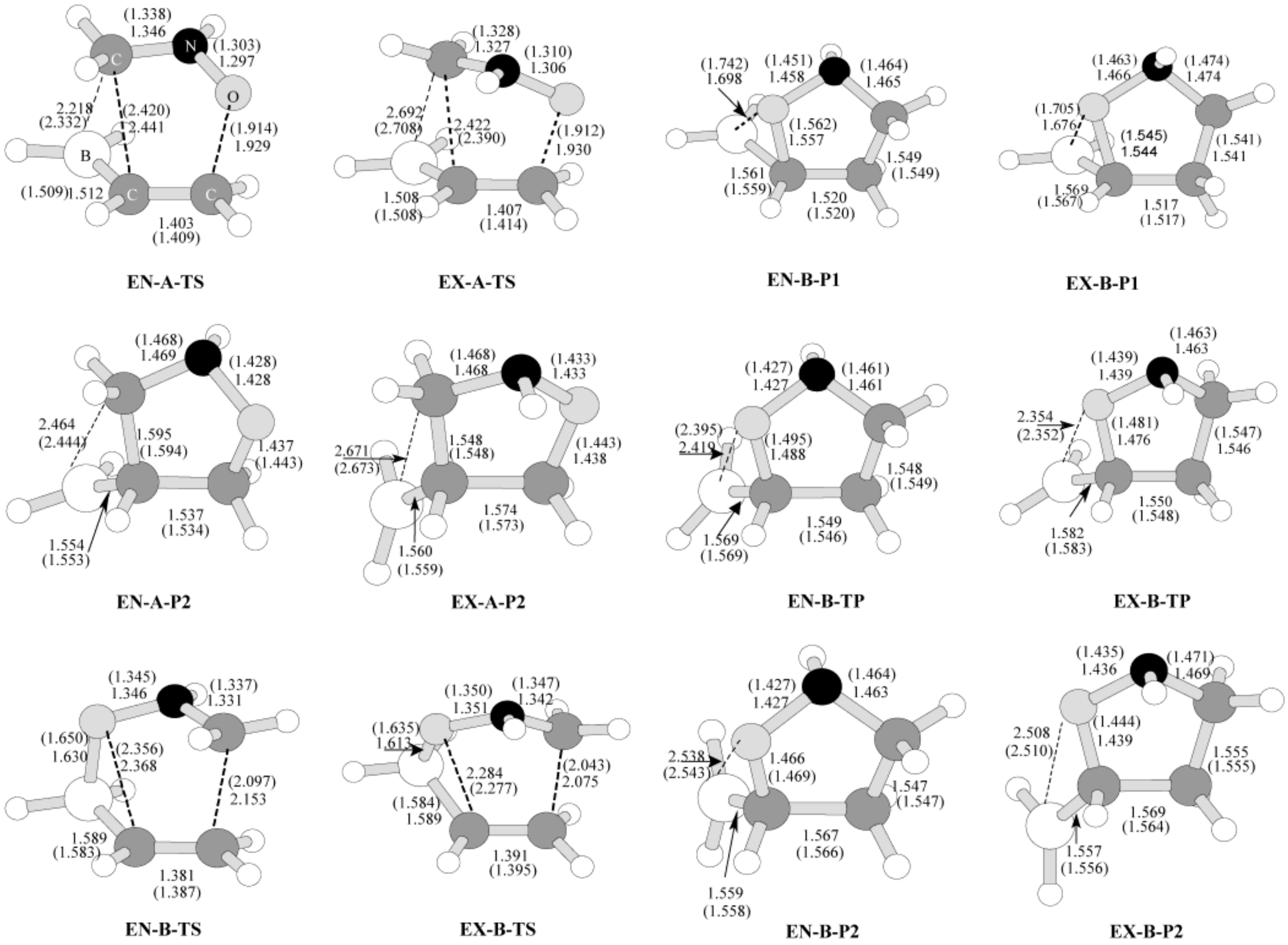

Figure 3. Optimized [B3LYP/6-31G(d), (MOD1)] stationary structures for the 1,3-dipolar cycloaddition of nitrone to vinylborane. Bond lengths are in angstroms. In parentheses are reported the B3LYP/AUG-cc-pVDZ (MOD2) values.

Table 1. Selected Distances (Å) and Corresponding Wiberg Bond Indices (italics) for the Stationary Structures of the Prototypical Cycloaddition (Vinylborane + Nitrone)

	MOD1[a] C···C		MOD2[b] C···C		MOD1[a] C···O		MOD2[b] C···O		MOD1[a] B···X		MOD2[b] B···X	
EN−B−C	4.911	*0.001*	4.933	*0.000*	2.606	*0.008*	2.613	*0.0061*	1.641	*0.516*	1.651	*0.509*
EX−B−C	3.644	*0.008*	3.672	*0.008*	2.617	*0.008*	2.620	*0.0107*	1.600	*0.561*	1.609	*0.534*
EN−B−TS	2.153	*0.383*	2.097	*0.423*	2.368	*0.136*	2.356	*0.1522*	1.630	*0.554*	1.650	*0.520*
EX−B−TS	2.075	*0.449*	2.043	*0.476*	2.284	*0.219*	2.277	*0.2333*	1.613	*0.554*	1.635	*0.516*
EN−A−TS	2.441	*0.231*	2.420	*0.255*	1.929	*0.451*	1.914	*0.4577*	2.218	*0.272*	2.332	*0.212*
EX−A−TS	2.421	*0.274*	2.390	*0.295*	1.930	*0.448*	1.912	*0.4583*	2.692	*0.097*	2.708	*0.091*
EN−B−P1	1.549	*0.984*	1.549		1.557	*0.761*	1.562		1.698	*0.435*	1.742	
EX−B−P1	1.541	*0.991*	1.541		1.544	*0.772*	1.545		1.676	*0.446*	1.705	
EN−B−TP	1.548	*0.984*	1.549		1.488	*0.869*	1.495		2.419	*0.089*	2.395	
EX−B−TP	1.546	*0.989*	1.547		1.476	*0.888*	1.481		2.354	*0.059*	2.352	
EN−B−P2	1.547	*0.987*	1.547		1.466	*0.888*	1.469		2.538	*0.035*	2.543	
EX−B−P2	1.555	*0.985*	1.555		1.439	*0.909*	1.444		2.508	*0.013*	2.510	
EN−A−P2	1.595	*0.932*	1.594		1.437	*0.913*	1.443		2.464	*0.060*	2.444	
EX−A−P2	1.548	*0.980*	1.548		1.438	*0.922*	1.443		2.671	*0.016*	2.673	

[a] MOD1 = B3LYP/6-31G(d). [b]MOD2 = B3LYP/AUG-cc-pVDZ.

The ENDO A reaction path provides a transition structure, **EN−A−TS**, at a fairly low energy as a consequence of the noteworthy B···C (2.218 Å, bond-index 0.27) interaction. Compared to the cycloaddition forming bonds (C···C, 2.441 Å, bond-index 0.23, and C···O 1.929 Å, bond-index 0.45), the B···C interaction, although about one-half of the B···O interaction in **EN−B-TS**, does justify the label (3 + 3 atoms) for **EN−A−TS**. IRC calculations directly connect **EN−A−TS** to the final product **EN−A−P2**. When **EN−A−TS** is launched toward reactants, IRC terminates to a complex with an energy slightly lower than that of the separated reactants; since (i) this stabilization is of the order of the counterpoise evaluation of the basis set superposition error, (ii) the geometries of the fragments are almost identical to those of the

---

(19) Isoxazolidenes **EN−B−P** and **EX−B−P** (**EN−A−P** and **EX−A−P**) can easily convert into each other by nitrogen inversion and ring flipping: Gandolfi, R.; Grünanger, P. Partially Saturated Polynuclear Isoxazoles. In *Isoxazoles*; Grünanger, P.; Vita Finzi, P., Eds.; Wiley-Interscience: New York, 1999; Part 2.

Table 2. Thermodynamic Relative Values (298.15 K) for the Prototypical Cycloaddition (Nitrone + Vinylborane)[a]

	MOD1			I[b]	MOD2			II[b]	III[b]	IV[b]	V[b]
	$\Delta H°$	$-\Delta S°$	$\Delta G°$	$\Delta G°$	$\Delta H°$	$-\Delta S°$	$\Delta G°$	$\Delta G°$	$\Delta G°$	$\Delta G°$	$\Delta G°$
reactants	0	0	0	0	0	0	0	0	0	0	0
EN−B−C	−16.79	28.0	−8.43	−10.54	−13.26	28.0	−4.90	−9.11	−9.78	−12.64	−4.99
EX−B−C	−15.51	31.4	−6.16	−8.85	−12.12	31.0	−2.87	−7.67	−7.20	−10.49	−3.01
EN−B−TS	−7.17	38.3	4.25	2.97	−1.97	38.1	9.39	2.98	4.83	1.75	10.82
EX−B−TS	−0.31	38.8	11.25	9.98	4.76	38.3	16.19	9.67	11.79	8.86	17.65
EN−A−TS	3.72	35.5	14.30	11.31	7.10	35.2	17.59	9.39	14.39	10.76	19.59
EX−A−TS	7.48	34.0	17.62	16.49	10.45	34.0	20.58	13.90	17.74	15.70	22.35
EN−B−P1	−26.11	38.8	−14.53	−21.43	−18.76	38.8	−7.19	−17.24			
EX−B− P1	−24.94	39.2	−13.26	−20.24	−17.69	39.2	−6.01	−15.85			
EN−B−TP	−22.06	37.7	−10.81	−14.61	−16.57	37.6	−5.36	−12.93			
EX−B−TP	−20.11	37.7	−8.88	−13.37	−14.78	37.1	−3.71	−11.84			
EN−B−P2	−22.15	35.0	−11.71	−16.08	−17.01	34.9	−6.61	−14.29			
EX−B−P2	−23.26	34.9	−12.85	−16.86	−18.07	34.9	−7.65	−15.26			
EN−A−P2	−22.63	35.8	−11.94	−15.90	−17.57	35.8	−6.88	−14.78			
EX−A−P2	−22.07	34.8	−11.70	−15.78	−16.89	34.8	−6.52	−14.46			

[a] MOD1 = B3LYP/6-31G(d), MOD2 = B3LYP/AUG-cc-pVDZ**;** Enthalpy and Free Enthalpy in kcal/mol; Entropy in cal/mol K. [b]Single-point calculations with kinetic contributions from MOD1 and MOD2: I, MP4/6-31G(d)//MOD1; II, MP4/AUG-cc-pVDZ//MOD2; III, B3LYP/cc-pVTZ//MOD2; IV, MP4/cc-pVDZ//MOD2; V, B3LYP/AUG-cc-pVTZ//MOD2.

separated reactants in the same model, and (iii) complex formation is certainly disfavored by entropy, we concluded that there is no evidence of a reactant complex in this case. **EXO−A−TS** transition structure reveals a comparatively very small $B\cdots C$ interaction (2.692 Å, bond-index 0.10), appears as a regular (3 + 2 atoms) structure, resides at a higher energy than **EN−A−TS**, and evolves toward reactants and products with the same features as **EN−A−TS**.

A-TSs can be described as the result of a nucleophilic attack by nitrone on the electron-poor vinylborane. Notice how in A-TSs the asynchronicity of forming bond lengths is reversed with respect to that in B-TSs, namely, in A-TSs, $C\cdots O$ bond formation is more advanced than $C\cdots C$ bond formation.

In conclusion, the $B\cdots X$ (X = O, C) interaction strongly determines the energy profile of the reaction, and in fact, it supplies very high reactivity toward nitrone cycloaddition and strongly supports the endo over the exo and the B over the A approach, thus providing a large preference for the ENDO B reaction path. In other words, it appears that the presence of the BH_2 substituent induces a sort of intramolecular catalysis that is also selective with respect to the different paths of 1,3-dipolar cycloaddition.[20]

Following the reaction with the MP4/MOD2 calculations does not alter the energy pattern. The MOD2 and MOD1 calculated geometries are very similar (Figures 1and 3) even though MOD2 (figures in parentheses) obtains slightly more “advanced” transition structures and slightly weaker $B\cdots X$ interactions than MOD1. The relative MP4/MOD2 energy values (in italics in Figure 2) are almost systematically higher than those of MP4/MOD1 except for the transition structures **EX−A−TS** and **EN−A−TS** which are located at lower energies, and for the structures **EX−B−TS** and **EN−B−TS** whose energies are very similar in the two models (Figure 2).

Table 2 presents the thermodynamic parameters for the reaction under study according to different kinds of calculations. Let us observe that the relative standard entropies are almost identical in the two models. Relative free enthalpies, on the contrary, are systematically much larger in MOD2 than in MOD1 B3LYP calculations; it is worth observing that the small differences in optimized geometries give only minor contributions to the differences in free enthalpies,[21] so that the large energy changes are bound to the difference of the two basis sets [6-31G(d) vs AUG-cc-pVDZ] in use with B3LYP density functional. With the aim of checking the level of reliability of the numerical values, we performed various single-point calculations using MOD1 and MOD2 geometries. When electron correlation is included via Moeller−Plesset post-SCF perturbation theory at the MP4(SDTQ) level (column I for MP4/6-31G(d)//MOD1 and column II for MP4/AUG-cc-pVDZ//MOD2, in Table 2), the results are reasonably alike and much more consistent with MOD1 than MOD2 B3LYP calculations; moreover, these results are also consistent with B3LYP/cc-pVDZ calculations (III) and MP4/cc-pVDZ//MOD2 (IV). So, it is only in those cases where the electronic energy is calculated with the B3LYP functional coupled with basis sets including diffuse functions (AUG-cc-pVDZ double-ζ and AUG-cc-pVTZ triple-ζ (column V in Table 2)) that much higher free enthalpies are systematically obtained. The same features have been found in the reaction of acrylonitrile with nitrone (Table 3); here again the presence of diffuse functions in the basis set both produces the highest activation free enthalpies in B3LYP calculations and gives rise to a strong decrease in activation free enthalpies on going from B3LYP to MP4 calculations, whereas in the absence of diffuse functions, B3LYP and MP4 calculations furnish similar results. The experimental activation parameters for the reaction of acrylonitrile with 1-pyrroline-1-oxide and 5,5-dimethyl-1-

---

(20) Lewis acid catalyzed, in particular with chiral catalysts, nitrone cycloadditions are under active investigation by several groups (Gothelf, K. V.; Jorgensen, K. A. *Chem. Rev.* **1998**, *98*, 863 and *Chem. Commun.* **2000**, 1449). Several examples in which the catalyst enhances reaction rates and selectivities of intermolecular cycloadditions by dipolarophile coordination have been reported (e.g., Kanemasa, S.; Oderaotoshi, Y.; Tanaka, J.; Wada, E. *J. Am. Chem. Soc.* **1998**, *120*, 12355. Simonsen, K. B.; Bayon, P.; Hazell, R. G.; Gothelf, K. V.; Jorgensen, K. A. *J. Am. Chem. Soc.* **1999**, *121*, 3845. Hori, K.; Kodama, H.; Ohta, T.; Furukawa, I. *J. Org. Chem.* **1999**, *64*, 5017). Less common are the examples in which an activating coordination between the nitrone oxygen and the Lewis acid is suggested (e.g., Ukaji, Y.; Taniguchi, K.; Sada, K.; Inomata, K. *Chem. Lett.* **1997**, 547. Seerden, J.-P.; Kuypers, M. M.; Scheeren, H. W. *Tetrahedron: Asymmetry* **1995**, *6*, 1441).

(21) For example, the free enthalpy of **EN−B−TS** changes from 4.25 kcal/mol in MOD1 to 9.39 in MOD2 (i.e., B3LYP/AUG-cc-pVDZ//MOD2) and to 9.41 in B3LYP/AUG-cc-pVDZ//MOD1; similarly, the free enthalpy of **EN−B−MP** changes from −14.53 to −7.19 and to −7.25 kcal/mol.

Table 3. Thermodynamic Relative Values (298.15 K) for the Reaction of Nitrone with Acrylonitrile[a]

	MOD1			I[b]	MOD2			II[b]
	$\Delta H°$	$-\Delta S°$	$\Delta G°$	$\Delta G°$	$\Delta H°$	$-\Delta S°$	$\Delta G°$	$\Delta G°$
EN−B−TS	10.05	33.3	19.95	17.66	13.58	33.0	23.41	14.77
EX−B−TS	10.90	33.2	20.78	18.49	14.06	32.9	23.88	15.33
EN−A−TS	10.07	33.6	20.09	19.58	13.02	33.7	23.06	16.07
EX−A−TS	10.97	33.8	21.05	20.92	13.96	33.8	24.05	17.47
apparent[c]	10.20	31.2	19.50					
apparent[d]	9.64	35.2	20.14					
EXP[e]	11.88	28.8	20.45					
EXP[f]	12.20	31.9	21.71					

[a] MOD1 = B3LYP/6-31G(d), MOD2 = B3LYP/AUG-cc-pVDZ; enthalpy and free enthalpy in kcal/mol; entropy in cal/mol K. [b] Single-point calculations: I, MP4/6-31G(d)//MOD1; II, MP4/AUG-cc-pVDZ//MOD2. [c] Calculated apparent activation parameters for the concomitant ENDOB, EXOB, ENDOA, EXOA reactions; when solvent effect (cyclohexane) is included, $\Delta G°$ raises to 20.50 kcal/mol. [d] For the reaction with 1-pyrroline-1-oxide; when solvent effect (cyclohexane) is included, $\Delta G°$ raises to 22.73 kcal/mol . [e] For the reaction with 1-pyrroline-1-oxide in cyclohexane. [f] For the reaction with 5,5-dimethyl-1-pyrroline-1-oxide in cyclohexane.

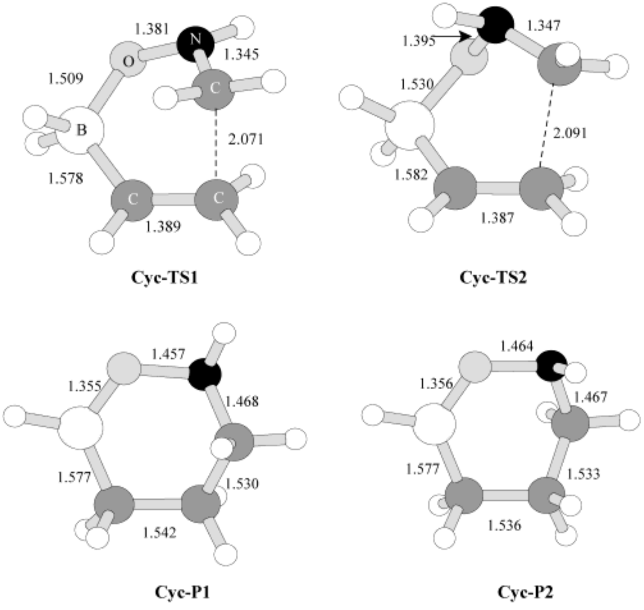

Figure 4. Optimized [B3LYP/6-31G(d)] stationary structures for cyclization reactions starting from **EN−B−C** and **EX−B−C** complexes. Bond lengths are in angstroms.

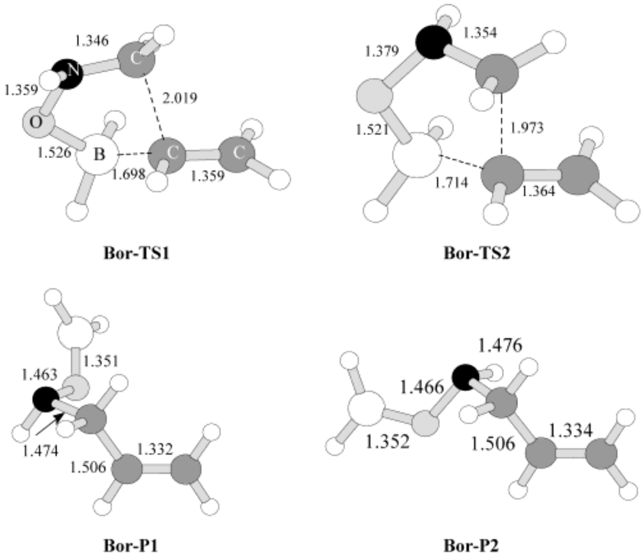

Figure 5. Optimized [B3LYP/6-31G(d)] stationary structures for boration reactions starting from **EN−B−C** and **EX−B−C** complexes. Bond lengths are in angstroms.

pyrroline-1-oxide in cyclohexane (15−35 °C)[3c,22] are shown in Table 3 to allow a comparison with the calculated values. Inspection of Table 3 clearly shows that theoretical data compare favorably with experimental findings.

Despite the variability of results of different calculations, the qualitative conclusions regarding the high reactivity of vinylborane−nitrone cycloaddition and the exclusive preference for ENDO B path are supported by all of the calculations presented.

Cyclization. Two transition structures (**Cyc-TS1**, **Cyc-TS2**) have been found (Figure 4) for the cyclization path; they are located at 1.98 and 3.60 kcal/mol above the reactant level and are connected by IRC calculations to the intermediate complex in the conformations **EN−B−C** and **EX−B−C** on one side, and to the very stable products **Cyc-P1** and **Cyc-P2** (oxazaborinane)[23] on the other side, where a hydrogen of the BH_2 underwent migration to the vicinal unsaturated carbon. An evident inflection on the IRC path seems to correspond to a dipolar intermediate (Scheme 1) (relative energy ca. 2.7 kcal/mol), which could not be singled out as a minimum.

Boration. Examples of competition between cycloaddition and 1,4-alkynylboration have been reported for the Diels−Alder reactions of 2-*tert*-butylbutadiene (2-phenylbutadiene) with alkynyldichloroboranes in dichloromethane yielding cyclohexadienes and enynes after protodeboronation with acetic acid and triethylamine.[24,25]

The search of concerted transition structures for boration led to the two structures, **Bor-TS1** and **Bor-TS2**, drawn in Figure 5. These structures have been found to be connected, by IRC calculations, to the reactant complexes **EX−B−C** and **EN−B−C**, respectively, on one side, and to the products **Bor-P1** and **Bor-P2** on the other side. The potential energy of **Bor-TS1** is 1.5 kcal/mol lower than that of **Bor-TS2** while **Bor-P2** is 0.9 kcal/mol more stable than **Bor-P1**.

Oxidation. At variance with the preceding reactions where cyclic transition structures are involved, oxidation is characterized by open transition structures. **Oxi-TS1** and **Oxi-TS2**, drawn in Figure 6, are two examples of possible Oxi-TSs leading to oxidated boranes and formaldimine by migration of hydrogen and vinyl group, respectively. On the side of products, IRC calculations seem to hesitate on oriented borane/formaldimine complexes which, by unrestricted optimization, collapse to the final products **Oxi-P1** and **Oxi-P2**. On the side of

---

(22) Scarpitta, F. Thesis, University of Pavia, 2000.

(23) **Cyc-P1** and **Cyc-P2** (**Bor-P1** and **Bor-P2**) can easily convert into each other by conformational rearrangements.

(24) Leung, S.-W.; Singleton, D. A. *J. Org. Chem.* **1997**, *62*, 1955.

(25) For a test of our calculation procedures, we have studied (Rastelli, A., unpublished results) the reactions (Diels−Alder and 1,4-alkynylboration) between butadiene and alkynyldichloroborane and found that in gas-phase and in cyclohexane the Diels−Alder reaction is largely dominant, whereas in dichloromethane boration becomes competitive as a consequence of solvent effects. Moreover, since the cycloaddition products are more stable than the alkynylboration products, we can expect that thermodynamic equilibration (long reaction times) should increase the content of cycloadditon products in the reaction mixture. All these results agree with experimental findings of ref 24.

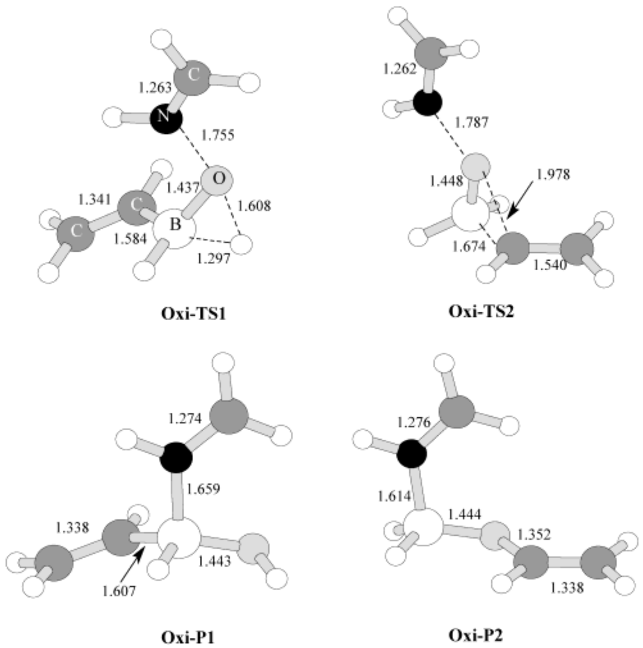

Figure 6. Optimized [B3LYP/6-31G(d)] stationary structures for oxidation reactions starting from **EN−B−C** and **C** complexes. Bond lengths are in angstroms.

reactants, IRC calculations show that **Oxi-TS2** evolves toward the **C** conformer of Figure 1, whereas **Oxi-TS1** evolves toward the **EN−B−C** conformer. One can see that the migration of the vinyl group (**Oxi-TS2**, **Oxi-P2**) requires higher activation energy than the migration of the H atom.

Competition among the Prototypical Reactions. Our results show that, according to the sequence of activation energies (1,3-dipolar cycloaddition ≪ boration < cyclization ≪ oxidation) (Figure 2 and BH$_2$ column of Figure 7), ENDO B cycloaddition (via paths b, d in Scheme 1) is the most favored among the reaction paths considered, although most of the transition structures appear easy to be reached under normal reaction conditions. The finding that the stability of reaction products shows a neatly reversed sequence could be relevant for the evaluation of the competition, and one might foresee that thermodynamic equilibration could even cause the absence of isoxazolidines among the reaction products. Moreover, solvent effects could influence the competition among the different reactions; a few rough evaluations[26] of the solvent effects ($\delta G_{\mathrm{sol}}^{\circ}$, CPCM) on the free enthalpies of reactants and transition structures are shown in Table 4 for toluene and dichloromethane. Although, according to actual values, solvent effects cannot modify the sequence of calculated activation free enthalpies, it does appear that they tend to foresee an increased relevance of boration, oxidation, and cyclization reactions in polar solvents.

In the following sections it will be investigated whether substitution on the prototypical reactants may significantly affect the pattern of TS relative energies.

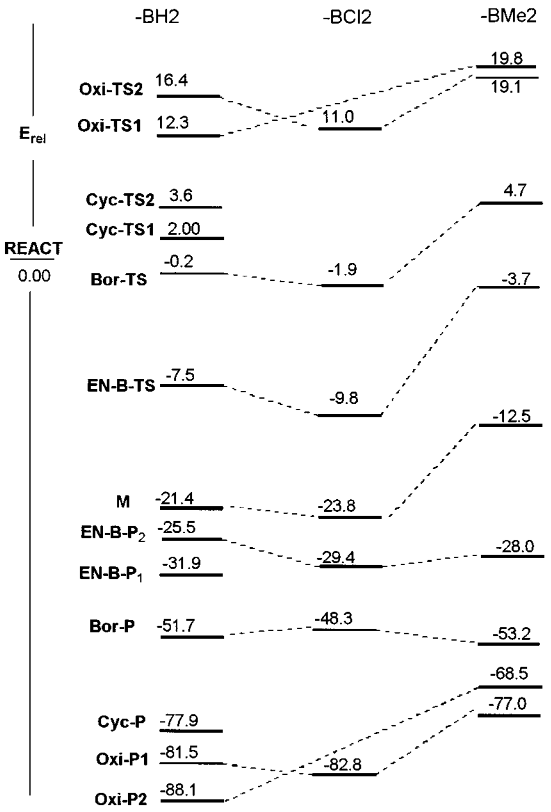

Figure 7. Substituent effects on the relative energy pattern of stationary structures for competing pathways of the reaction of nitrone with vinylboranes ($CH_2{=}CH{-}BX_2$). MP4(SDTQ)/6-31G(d)//B3LYP/6-31G(d) energies including ZPE contributions.

Table 4. Electrostatic Solvent Effect ($\delta G_{\mathrm{sol}}^{\circ}$, CPCM) for TSs of the Competing Paths in the Reaction of Nitrone with Vinylborane in Toluene and Dichloromethane[a]

structure	toluene	CH_2Cl_2	structure	toluene	CH_2Cl_2
nitrone	−2.77	−4.43	**Cyc-TS1**	−3.99	−6.55
vinylborane	−0.30	−0.48	**Cyc-TS2**	−3.45	−5.65
EN−B−TS	−3.84	−6.24	**Bor-TS1**	−4.65	−7.60
EX−B−TS	−4.12	−6.73	**Bor-TS2**	−4.18	−6.84
EN−A−TS	−2.56	−4.08	**Oxi-TS1**	−4.21	−6.84
EX−A−TS	−2.54	−4.07	**Oxi-TS2**	−4.49	−7.25

[a] MOD1 = B3LYP/6-31G(d); $\delta G_{\mathrm{sol}}^{\circ}$ in kcal/mol

Substituent Effects. (a) 1,3-Dipolar Cycloaddition. To investigate the role of steric and electronic substituent effects and to characterize the class of reactions, we have considered chloro and methyl substitution for hydrogens of the BH$_2$ group (i.e., dichlorovinylborane and dimethylvinylborane, respectively), methyl substitution on the C-1 atom (i.e., 2-propenylborane) and dimethyl substitution on the C-2 atom of the vinyl group (i.e., 2-methyl-1-propenylborane), and methyl substitution on the N atom of the nitrone. The results are collected in Table 5 and Figure 7. Let us underline the most relevant pieces of information: (i) the free enthalpy sequence of transition structures remains unaltered with respect to the prototypical reaction, ENDO B path always resulting in the preferred one; (ii) the substitution of two methyl groups for hydrogens in BH$_2$ strongly enhances the activation free enthalpy of **EN−B−TS**, in parallel with a weaker B···O interaction (1.714 vs 1.630 Å); the reactivity of dimethylvinylborane toward nitrone, however, still remains much higher than that of acrylonitrile (Table 3); (iii) also dimethyl substitution on the C-2 center of the reacting vinyl group (i.e., on passing from vinylborane to 2-methyl-1-propenylborane) strongly enhances the activation free enthalpy of **EN−B−TS**, but, in this

---

[26] We have used CPCM procedure of ref 15, but we report only the electrostatic term because the parameters for the evaluation of nonelectrostatic contributions of the boron atom are missing.

Table 5. Thermodynamic Parameters (298.15 K) for the TSs of the Reactions of Nitrone with Substituted Vinylboranes and *N*-Methylnitrone with Vinylborane[a]

	MOD1				I[b]	MOD2			
	ΔH°	$-\Delta S^\circ$	ΔG°	B···X	ΔG°	ΔH°	$-\Delta S^\circ$	ΔG°	B···X
				$CH_2{=}CH{-}BMe_2$ + Nitrone					
EN−B−TS	0.69	43.0	13.50	1.714	8.23	5.96	42.5	18.62	1.761
EX−B−TS	7.92	42.5	20.60	1.741	15.14				
EN−A−TS	8.57	37.7	19.81	2.641	16.31	11.49	36.1	22.24	2.671
				$CH_2{=}CH{-}BH_2$ + *N*-Methyl Nitrone					
EN−B−TS	−4.73	38.7	6.80	1.663	3.59				
EX−B−TS	−1.07	39.7	10.75	1.622	7.12				
EN−A−TS	4.19	36.1	14.95	2.310	10.62				
EX−A−TS	7.19	34.5	17.48	2.672	14.78				
				$CH_2{=}CMe{-}BH_2$ + Nitrone					
EN−B−C	−19.57	32.1	−9.99	1.651	−13.17				
EN−B−TS	−10.40	38.5	1.08	1.616	−0.92	−5.71	38.2	5.67	1.629
EN−A−TS	3.03	37.2	14.11	1.951	9.40	6.88	36.4	17.71	2.020
				$CMe_2{=}CH{-}BH_2$ + Nitrone					
EN−B−TS	−1.04	41.0	11.18	1.605	5.79				
				$CH_2{=}CH{-}BCl_2$ + Nitrone					
EN−B−TS	−7.20	35.1	3.26	1.570	0.72	0.75	39.8	12.61	1.583
EX−B−TS	1.88	35.2	12.37	1.575	10.10				
EN−A−TS	3.21	29.7	12.05	2.773	10.24	8.82	34.5	19.11	2.783
				$CMe_2{=}CH{-}BCl_2$ + Nitrone					
EN−B−TS	1.11	47.4	15.23	1.545	8.44				

[a] MOD1= B3LYP/6-31G(d), MOD2 = B3LYP/AUG-cc-pVDZ; enthalpy and free enthalpy in kcal/mol; entropy in cal/mol K. [b] Single-point calculations with kinetic contributions from MOD1: I, MP4/6-31G(d)//MOD1.

case, the B···O interaction becomes stronger (1.605 vs 1.630 Å) and the forming C···C bond shorter (2.035 vs 2.153 Å), thus indicating that the steric hindrance of the methyl groups causes a less early transition structure; (iv) the *N*-methyl substitution of nitrone causes a small increase of **EN−B−TS** activation free enthalpy and a small decrease of the B···O interaction (1.663 vs 1.630 Å); (v) interestingly, the presence of a methyl group in 2-propenylborane strongly increases the ENDO B reactivity, while leaving unaltered the ENDO A reactivity. In this case, however, the B···O interaction is only slightly increased (1.617 vs 1.630 Å); (vi) dichlorovinylborane shows a very high ENDO B reactivity, higher than that of vinylborane, and a much shorter B···O distance, in agreement with the higher electrophilicity of BCl_3 with respect to BH_3; here again, dimethyl substitution on the C2 reacting center (2-methyl-1-propenyldichloroborane) strongly increases the activation free enthalpy of **EN−B−TS** as a consequence of a much more advanced transition structure (B···O distance 1.545 Å, C···C forming bond 1.953 Å).

Substituent Effects. (b) Competition among the Reactions. Also the transition structures found for boration and oxidation of dichlorovinylborane and dimethylvinylborane are quite similar to those found for vinylborane. As for cyclization, we could not locate with sufficient accuracy the ring closure structures because they happened to merge with the 1,3-cycloaddition structures. Figure 7 collects the activation energies [MP4-(SDTQ)/6-31G(d)//B3LYP/6-31G(d)] of the reactions of dichlorovinylborane ($-BCl_2$) and dimethylvinylborane ($-BMe_2$) in comparison with the relative energies of the most stable stationary structures of vinylborane ($-BH_2$). One can remark that (i) 1,3-cycloaddition and boration are similarly affected by boron substitution so that their activation energies maintain the same gap (>7 kcal/mol) in favor of the former reaction; (ii) the energy gap between 1,3-cycloaddition and oxidation transition structures is very high (>20 kcal/mol); the transition structure **Oxi-TS1**, not found for the oxidation of dichlorovinylborane, has been located at higher energy than **Oxi-TS2** for dimethylvinylborane: this probably suggests that, at variance with vinylborane, oxidation of dimethylvinylborane should favor the migration of the vinyl group, and oxidation of dichlorovinylborane should occur only with migration of the vinyl group. For the rest, it appears that competition among the different reactions is not qualitatively affected by the substituent effects considered here.

The dimethyl substitution on the C-2 center of vinylborane (2-methyl-1-propenylborane and 2-methyl-1-propenyldichloroborane), on the contrary, other than causing a high increase of activation free enthalpy for the 1,3-dipolar cycloaddition, does produce relatively low activation free enthalpy for the boration reaction (6.86 and 8.46 kcal/mol, respectively, to be compared with 5.79 and 8.44 kcal/mol for the 1,3-cycloaddition, Table 5), so that competition of boration with cycloaddition appears to be very likely also in the gas-phase. Setting the comparison in the terms of Figure 7, i.e., using MP4(SDTQ)/6-31G-(d)//B3LYP/6-31G(d) activation energy including ZPE contributions, it is found that 1,3-cycloaddition is favored over boration by only 1.94 kcal/mol with 2-methyl-1-propenylborane and 1.17 kcal/mol with 2-methyl-1-propenyldichloroborane.

Conclusions

The results of this investigation coherently support the conclusion that vinylboranes and simple substituted vinylboranes may undergo very fast 1,3-dipolar cycloaddition to nitrones resulting in single adducts which are the *endo*-5-borylisoxazolidines. The boryl substituent is intimately involved in the reaction mechanism via very strong B···O interactions able to produce very low energy barriers, regiospecifity and complete endo-stereoselectivity, in a sort of effective and selective intramolecular catalysis. Although boration is a fast reaction and oxidation is also an accessible route, according to the calculated activation energies in vacuo, they do not appear to be competitive with 1,3-cycloaddition on the grounds of *kinetic control*, at least when the C-2 atom of vinylborane is left unsubstituted.

Several other aspects should be explored in order to get real a priori predictions, but, in our opinion, the present study should offer sufficient basis and arguments for understanding the outcome of experimental reactions and for justifying the effort of making experimental tests.

Actually, experimental results are necessary in order to (i) either confirm (partially or *in toto*) the theoretical reaction scheme and (ii) provide valuable input for further theoretical work, or (iii) produce precious criticism to the theoretical models which are currently and successfully used to rationalize the already known experimental facts in the field of Diels–Alder reactions and 1,3-dipolar cycloadditions.

Acknowledgment. We thank MURST for financial support and CICAIA (University of Modena) for computer facilities.

JO001801N